



UNIVERSITY
OF TRENTO

DIPARTIMENTO DI INGEGNERIA E SCIENZA DELL'INFORMAZIONE

38123 Povo – Trento (Italy), Via Sommarive 14
<http://www.disi.unitn.it>

OPTIMIZATION OF A SPLINE-SHAPED UWB ANTENNA BY PSO

L. Lizzi, F. Viani, R. Azaro, and A. Massa

January 2011

Technical Report # DISI-11-003

Optimization of a Spline-Shaped *UWB* Antenna by *PSO*

Leonardo Lizzi, Federico Viani, Renzo Azaro, and Andrea Massa,

Abstract

This letter presents the design of a planar antenna for *UWB* applications with a bandwidth of **5.5 GHz** over **3.7 to 9.2 GHz** and return loss values lower than -10 dB. The antenna geometry is described in terms of a spline-based representation whose control parameters, together with other geometrical descriptive quantities, are determined through a suitable Particle Swarm optimizer (*PSO*) in order to fit the *UWB* requirements. Representative results of both numerical and experimental validations are reported in order to assess the performance of the prototype as well as to give some preliminary indications on the reliability and effectiveness of the whole synthesis approach.

Index Terms

Antenna Synthesis, Ultra-Wide-Band (*UWB*), Particle Swarm Optimizer (*PSO*), Splines.

I. INTRODUCTION

Ultra-wideband (*UWB*) radio is an emerging technology with attractive features useful for wireless communications, networking, radar processing, imaging, and positioning systems [1].

While often ignored or assumed with an ideal behavior in dealing with conventional narrow-band communication systems, antennas are a critical element in the signal flow of *UWB* systems. In such a context, antennas play a relevant role because of their “bandpass filter” behaviors and/or the arising undesired distortions if not properly designed. On the other hand, an optimized synthesis aimed at fitting frequency-domain parameters (i.e., return loss, gain, radiation patterns and polarization, in addition to bandwidth) is not enough to guarantee suitable antenna performances for *UWB* applications, since these quantities might significantly vary in the whole *UWB* band causing a wrong or perturbed transmission and reception of pulses. For such a reason, traditional approaches to antenna characterization prove to be inadequate. Therefore, *UWB* radiators should be examined from a different perspective for providing a proper and accurate description of the antennas behaviors [2]. Consequently, customized synthesis techniques are needed [3].

Unlike narrow-band systems, both transmitting and receiving antenna [4] not only affect pulses amplitudes, but also cause non-negligible distortions to the signal waveform. Therefore, the *UWB* antenna design is usually aimed at satisfying the following requirements: (a) a good impedance matching over the whole operating bandwidth; (b) the *UWB* transmitting/receiving system is a distortionless system.

Towards this purpose, a number of different antennas designs have been proposed. For example, the diamond and rounded diamond antennas described in [5], the annular ring antenna proposed by *Ren and Chang* in [6], the microstrip notched antenna with fractal stub in [7], and monopole antennas in [8][9].

In this letter, unlike standard techniques aimed at matching only impedance bandwidth and radiation properties, the antenna is the result of a full approach that takes into account all the *UWB* specifications including the distortionless properties of an *UWB* system constituted by a couple of identical antennas that simulate an *UWB* propagation channel. Towards this end, the arising optimization problem is addressed by means of an integrated strategy whose building blocks are a spline-based shape generator [10] and a *PSO* procedure [11]. More in detail, the positions of a limited set of “control points” are determined and used for generating, by using the spline-based generator (*SG*), the contours of a set of trial antennas. Such trial configurations are ranked according to the matching of their electrical characteristics (computed by means of a *MoM* simulator) with the specifications and iteratively updated through the *PSO* logic until all the requirements are satisfied.

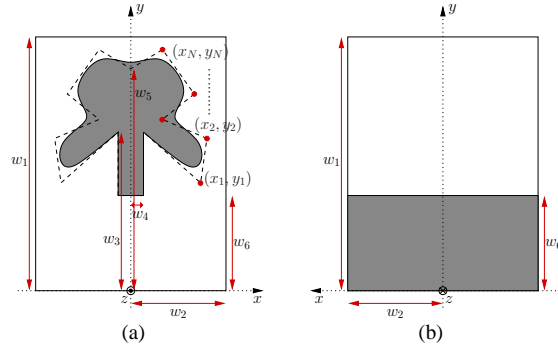


Fig. 1. Antenna descriptive parameters - (a) front view and (b) back view.

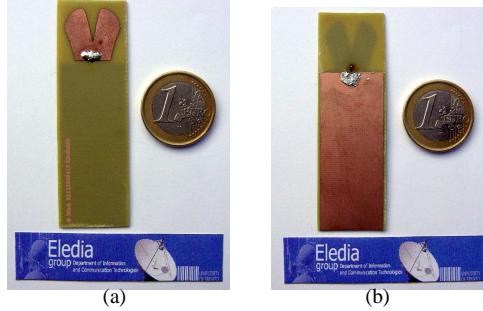


Fig. 2. Antenna prototype - (a) front view and (b) back view.

The paper is organized as follows. In Section 2, the synthesis problem is formulated and recasts as the optimization, through the *PSO* strategy, of a suitable cost function that depends on a spline-based representation of the antenna shape. Then, a set of representative results are reported in order to numerically and experimentally assess the efficiency of the synthesized prototype as well as (although preliminary) the reliability of the synthesis methodology (Sect. 3). Finally, some conclusions are drawn (Sect. 4).

II. ANTENNA DESIGN

The design of the *UWB* microstrip antenna is formulated as an optimization problem aimed at defining a set of representative geometrical variables in order to satisfy suitable requirements/constraints on the electrical behavior in the *UWB* bandwidth.

Figure 1 shows the representative parameters to be optimized. Since a symmetry condition along the $y - z$ plane of the antenna structure is assumed, only half of the physical structure is modeled and therefore the antenna geometry turns out to be completely characterized by the following array of geometric variables

$$\bar{x} = \{(x_n, y_n), n = 1, \dots, N; w_1, w_2, \dots, w_6\} \quad (1)$$

where the coordinates of the n -th control point of the spline-based representation are denoted by (x_n, y_n) , $n = 1, \dots, N$, N being the total number of control points used to unambiguously describe the antenna geometry. Moreover, w_1 is the substrate length, w_2 is one half of the substrate width, w_4 one half of the feed-line width, w_6 the length of the ground-plane, and w_3 and w_5 defines the range of contour variations along the y -axis (as shown in Fig. 1).

As far as the *UWB* requirements are concerned, the electrical conditions previously formulated are resumed in the following set of constraints. Concerning the impedance matching over the bandwidth of the considered *UWB* device [15],

$$|S_{11}(f)| \leq |\widetilde{S}_{11}(f)| = -10 \text{ dB} \quad f_1 \leq f \leq f_2 \quad (2)$$

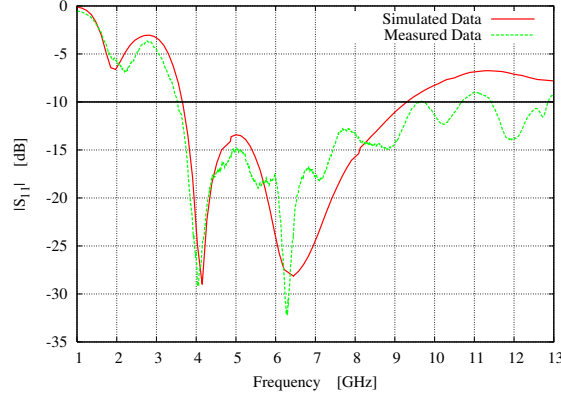


Fig. 3. Numerical and experimental assessment - Amplitude of S_{11} vs. frequency.

where $f_1 = 4 \text{ GHz}$ and $f_2 = 9 \text{ GHz}$ and the superscript \sim indicates the reference value. Moreover, as regards to the condition of distortionless system, the antenna is required to satisfy a condition on the magnitude of S_{21} , $|S_{21}(f)|$,

$$\Delta |S_{21}| \leq \widetilde{\Delta |S_{21}|} = 6 \text{ dB} \quad (3)$$

being $\Delta |S_{21}| = \max_{f_1 \leq f \leq f_2} \{|S_{21}(f)|\} - \min_{f_1 \leq f \leq f_2} \{|S_{21}(f)|\}$, and on the group delay τ_g

$$\Delta \tau_g \leq \widetilde{\Delta \tau_g} = 1 \text{ ns} \quad (4)$$

where $\Delta \tau_g = \max_{f_1 \leq f \leq f_2} \{\tau_g(f)\} - \min_{f_1 \leq f \leq f_2} \{\tau_g(f)\}$, being $\tau_g(f) = -\frac{d}{df} \{\angle S_{21}(f)\}$. Finally, the antenna is required to belong to a physical platform of dimension $100 \times 60 \text{ mm}^2$.

Starting from such specifications, the unknown descriptive array (1) is determined by minimizing the following cost function

$$\Psi(\bar{x}) = \Psi_{11}(\bar{x}) + \Psi_{21}(\bar{x}) + \Psi_{GD}(\bar{x}) \quad (5)$$

where

$$\Psi_{11}(\bar{x}) = \int_{f_1}^{f_2} \max \left\{ 0, \frac{|S_{11}(f)| - \widetilde{|S_{11}(f)|}}{\widetilde{|S_{11}(f)|}} \right\} df \quad (6)$$

$$\Psi_{21}(\bar{x}) = \max \left\{ 0, \frac{\Delta |S_{21}| - \widetilde{\Delta |S_{21}|}}{\widetilde{\Delta |S_{21}|}} \right\} \quad (7)$$

$$\Psi_{GD}(\bar{x}) = \max \left\{ 0, \frac{\Delta \tau_g - \widetilde{\Delta \tau_g}}{\widetilde{\Delta \tau_g}} \right\} \quad (8)$$

Towards this end, a suitable implementation of the *PSO* [12] has been integrated with a spline-based shape generator and a *MoM*-based [13] electromagnetic simulator. Each trial solution $\bar{x}_p^{(k)}$ ($p, p = 1, \dots, P$, and $k, k = 0, \dots, K$, being the trial index and the iteration index, respectively) identifies an antenna structure, $A_p^{(k)}$, determined by applying the *SG* (i.e., $A_p^{(k)} = SG \{ \bar{x}_p^{(k)} \}$). The electric parameters of such a trial antenna are computed by means of the *MoM* simulator in order to evaluate its fitting $\Psi_p^{(k)} = \Psi(\bar{x}_p^{(k)})$ with the project specifications. The set of P solutions is iteratively updated by modifying antennas descriptions ($\bar{x}_p^{(k)} \leftarrow \bar{x}_p^{(k+1)}$; $p = 1, \dots, P$) through the *PSO*, until $k = K$ or $\Psi^{opt} \leq \eta$ (η being the convergence threshold and $\Psi^{opt} = \min_k \{ \min_p [\Psi_p^{(k)}] \}$).

III. NUMERICAL SIMULATION AND EXPERIMENTAL VALIDATION

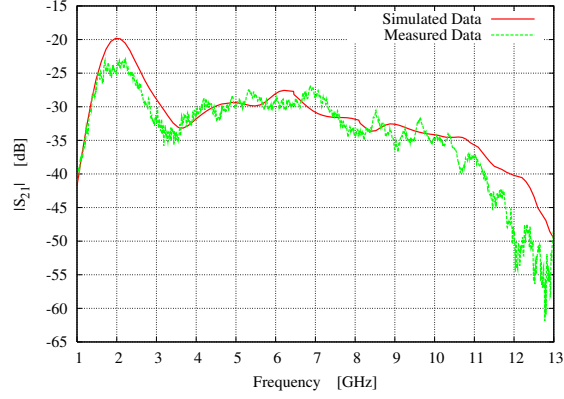


Fig. 4. Numerical and experimental assessment - Amplitude of S_{21} vs. frequency.

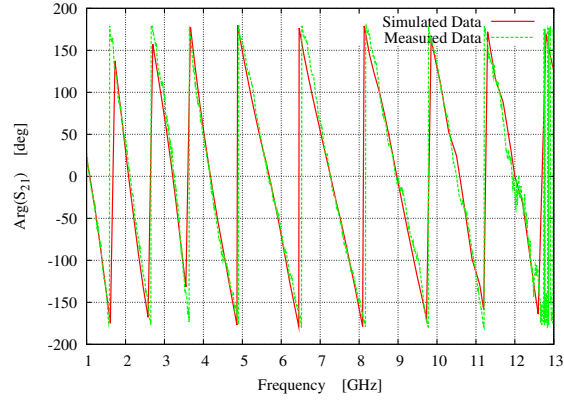


Fig. 5. Numerical and experimental assessment - Phase of S_{21} vs. frequency.

As far as the PSO setup is concerned, the following parameter configuration has been chosen: $P = 7$ trial solutions, $\eta = 10^{-5}$, and $K = 600$. Moreover, an Arlon layer of 0.78 mm thickness ($\epsilon_r = 3.38$) has been assumed as substrate and $N = 5$ control points have been used for the antenna description.

After the optimization, the synthesized antenna belongs to a surface of dimensions $w_1 = 69.2\text{ mm}$ in length and $w_2 = 10\text{ mm}$ in width and the following values for the control points have been obtained: $x_1 = 6.9\text{ mm}$, $y_1 = 50.6\text{ mm}$, $x_2 = 9\text{ mm}$, $y_2 = 55.5\text{ mm}$, $x_3 = 7\text{ mm}$, $y_3 = 62.7\text{ mm}$, $x_4 = 2.7\text{ mm}$, $y_4 = 66.3\text{ mm}$, $x_5 = 1.9\text{ mm}$, $y_5 = 61.8\text{ mm}$. Moreover, $w_4 = 5.4\text{ mm}$, $w_3 = 51.6\text{ mm}$, $w_5 = 56\text{ mm}$, and $w_6 = 51\text{ mm}$. Accordingly, the antenna prototype has been built using a photo-lithographic printing circuit technology (Fig. 2) and it has been equipped with a SMA connector and fed with a coaxial line. The electrical parameters have been measured by using an Anritsu Vector Network Analyzer (37397D Lightning) in a non-controlled environment and, concerning the measurement of S_{21} values, a distance of 15 cm between the two equal (Tx/Rx) antenna prototypes has been chosen [14].

Figure 3 shows the simulated and measured values of $|S_{11}|$. As it can be observed, the behavior of the synthesized antenna fits the guidelines from $f = 3.7\text{ GHz}$ up to $f = 9.2\text{ GHz}$ (i.e., within the Federal Communication Commission mask [15]), considering both simulated and measured data, and the antenna bandwidth turns out to be 5.5 GHz (i.e., a fractional bandwidth equal to 85.3 %). Moreover, the widest variation of the magnitude of S_{21} is less than 5 dB (Fig. 4). For completeness, the values of the phase of S_{21} are also reported in Fig. 5.

As far as the group delay is concerned, the plots in Fig. 6 show a nearly constant trend in correspondence with simulated data

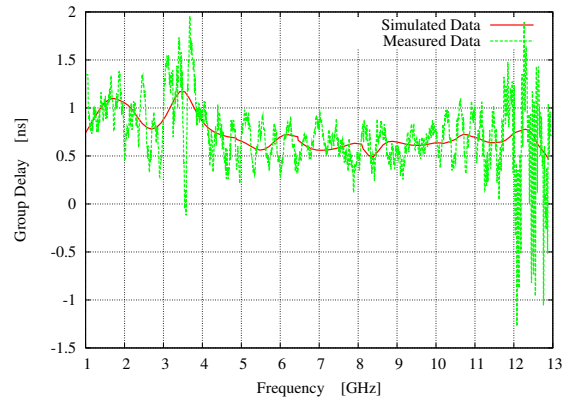


Fig. 6. Numerical and experimental assessment - Group delay τ_g vs. frequency.

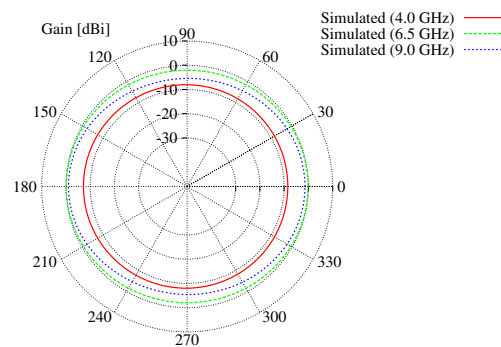


Fig. 7. Numerical assessment - Radiation pattern on the $x - z$ plane.

(the widest variations being less than 0.5 ns), while, even though in a reasonable accordance with simulations, the measured behavior presents larger fluctuations that might be attributed to the non-controlled measurement environment.

Finally, some samples of the numerically-computed radiation patterns at different frequencies ($f_a = 4.0 \text{ GHz}$, $f_b = 6.5 \text{ GHz}$, and $f_c = 9.0 \text{ GHz}$) on the $x - z$ plane (Fig. 7) and on the $x - y$ plane (Fig. 8) are shown. As it can be noticed, the antenna approximately behaves as omnidirectional radiator in the horizontal plane, while a monopolar-like behavior appears in the vertical section since lower gain values turns out at 0° and 180° .

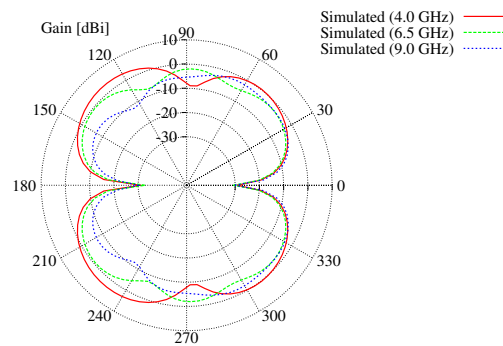


Figure 8: Numerical assessment - Radiation pattern on the $x - y$ plane.

IV. CONCLUSION

In this letter, the synthesis of a new spline-shaped *UWB* antenna has been presented. The antenna is the result of the application of an innovative design approach based on the use of a spline description for the antenna geometry and of a formulation of the synthesis in terms of return loss at the input port and coupling properties of a system of identical antennas modeling the *UWB* communication. In order to verify the efficiency of the optimized antenna as well as (in a preliminary fashion) the effectiveness and reliability of the design methodology, a prototype has been built. The measured electrical parameters confirm the reliability of the antenna as well as the matching with *UWB* project guidelines.

REFERENCES

- [1] L. Yang and G. B. Giannakis, "Ultra-wideband communications," *IEEE Signal Processing Mag.*, pp. 26-54, Nov. 2004.
- [2] X. Qing, Z. N. Chen, and M. Y. W. Chia, "Characterization of ultrawideband antennas using transfer functions," *Radio Sci.*, vol. 41, RS1002, 2006.
- [3] Z. N. Chen, X. H. Wu, H. F. Li, N. Yang, and M. Y. W. Chia, "Consideration for source pulses and antennas in UWB radio system," *IEEE Trans. Antennas Propagat.*, vol. 52, no. 7, pp. 1739-1748, Jul. 2004.
- [4] X. H. Wu and Z. N. Chen, "Design and optimization of UWB antennas by a powerful CAD tool: PULSE KIT," *IEEE Antennas Propagat. Int. Symp.*, vol. 2, pp. 1756-1759, Jun. 2004.
- [5] G. Lu, S. von der Mark, I. Korisch, L. J. Greenstein, and P. Spasojevic, "Diamond and rounded diamond antennas for ultrawide-band communications," *IEEE Antennas Wireless Propagat. Lett.*, vol. 3, pp. 249-252, 2004.
- [6] Y. Ren and K. Chang, "An annular ring antenna for UWB communications," *IEEE Antennas Wireless Propagat. Lett.*, vol. 5, pp. 275-276, 2006.
- [7] W. J. Lui, C. H. Cheng, Y. Cheng and H. Zhu, "Frequency notched ultra-wideband microstrip slot antenna with fractal tuning stub," *Electronics Letters*, vol. 41, no. 6, Mar. 2005.
- [8] J. Jung, W. Choi and J. Choi, "A small wideband microstrip-fed monopole antenna," *IEEE Microwave Wireless Components Lett.*, vol. 15, no. 10, pp. 703-705, Oct. 2005.
- [9] J. Liang, C. C. Chiau, X. Chen and C. G. Parini, "Study of a printed circular disc monopole antenna for uwb systems," *IEEE Trans. Antennas Propagat.*, vol. 53, no. 11, pp. 3500-3504, Nov. 2005.
- [10] C. de Boor, *A Practical Guide to Spline*. Springer, New York, 2001.
- [11] J. Robinson and Y. Rahmat-Samii, "Particle Swarm Optimization in Electromagnetics," *IEEE Trans. Antennas Propagat.*, vol. 52, no. 2, Feb. 2004.
- [12] R. Azaro, F. De Natale, M. Donelli, A. Massa, and E. Zeni, "Optimized design of a multi-function/multi-band antenna for automotive rescue systems," *IEEE Trans. Antennas Propagat.*, vol. 54, no. 2, pp. 392-400, Feb. 2006.
- [13] R. F. Harrington, *Field Computation by Moment Methods*. Malabar, FL: Robert E. Krieger, 1987.
- [14] S. H. Lee, J. K. Park, and J. N. Lee, "A novel CPW-fed ultra-wideband antenna design," *Microwave Optical Technology Lett.*, vol. 44, no. 5, Mar. 2005.
- [15] Federal Communications Commission, First Report and Order, "Revision of part 15 of the commission's rules regarding ultra-wideband transmission systems," *FCC 02-48*, Apr. 2002. http://hraunfoss.fcc.gov/edocs_public/attachmatch/FCC-02-48A1.pdf